SolarPACES 2024, 30th International Conference on Concentrating Solar Power, Thermal, and Chemical Energy Systems

Power Cycles

https://doi.org/10.52825/solarpaces.v3i.2331

Published: 21 Nov. 2025

Comparison of Shell and Tube Heat Exchangers for CO_2 and CO_2+$SiCl_4$ Mixtures Transcritical Cycles

Vladimir Naumov[1], Marta Mantegazza[2], Michele Doninelli[1], Gioele Di Marcoberardino[1], Paolo Iora[1], and Marco Rottoli[2]

[1]Università degli studi di Brescia, Brescia, Italy

[2]Brembana & Rolle S.P.A, Valbrembo (BG), Italy

*Correspondence: Vladimir Naumov, vladimir.naumov@unibs.it

Abstract. Concentrated solar power (CSP) plants have great potential for clean energy production, but their electricity cost is higher than that of noncontrollable renewable energy sources. The main ways to lower the electricity cost are equipment cost reduction and plant efficiency increase. Looking at the power unit, the closed supercritical CO_2 (sCO_2) cycles offer the efficiency advantage over both the steam Rankine and helium Brayton cycles at high turbine inlet temperatures. Further improvement could be achieved by increasing the critical temperatures using mixtures, allowing condensation at temperatures typical for air-cooled condensers. The sCO_2 and CO_2 mixture cycles are significantly affected by the performance of the recuperative system and require high pressures (comparable to steam cycles). An increase in efficiency compensates for higher complexity in the design and construction of the plant, according to the authors. High thermal power together with high pressures and temperatures demand customized CO_2 heat exchanger designs, which makes them a major part of power cycle specific cost. This paper provides a robust technological solution for the implementation of the above cycles in an industrial setup based on shell-and-tube heat exchangers. Based on the thermohydraulic and mechanical design of EMbaffle® Technology, heat exchangers weight reduction can be quantified in the range of 30 to 60% depending on the application, with additional advantages in terms of logistics and installation (footprint, foundations, etc…). Using the CO_2+$SiCl_4$ mixture instead of pure sCO_2 leads to a lower weight of primary and high-temperature heat exchangers, while the weight of low-temperature heat exchanger increases.

Keywords: Shell and Tube Heat Exchanger, sCO_2, CO_2+$SiCl_4$ Mixture, Trans-Critical Cycle, EMbaffle, No Tube in Window

1. Introduction

Concentrated solar power (CSP) plants generate thermal power as an intermediate step between solar radiation and electricity and therefore can use cheap thermal energy storage. This makes them a flexible dispatchable source of renewable energy. However, the actual cost of electricity from CSP plants is higher than from photovoltaic or wind power plants [1], but their power generation depends on weather conditions and is uncontrollable. The CSP electricity cost reduction can be pursued by reducing the cost of equipment and increasing the generation efficiency. The closed supercritical CO_2 (sCO_2) cycles offer an efficiency advantage over both the steam Rankine and helium Brayton cycles at turbine inlet temperature (TIT) > 600°C [2]. One of the ways to improve their efficiency is to move towards the CO_2 mixture cycles, which have higher critical temperatures and allow condensation even at 50°C [3]. To improve the

sCO_2 cycle performance, a $SiCl_4$ dopant, which could be stable up to 900°C [4], has been considered. Bubble points and liquid density of the CO_2+$SiCl_4$ mixture have recently been measured by Doninelli et al. [5] allowing for the calculation of cycle performance: the use of a CO_2+$SiCl_4$ mixture instead of sCO_2 increased the efficiency of the recompression cycle at 700°C TIT by 1.3%. Pure $SiCl_4$ thermal conductivity and viscosity have been accurately modeled using the friction theory [6], [7] therefore allowing for the characterization of the heat exchangers performance. The sCO_2-based cycles are significantly affected by the recuperative system and require high pressures (comparable to supercritical steam cycles). High thermal power together with high pressures and temperatures leads to sCO_2 heat exchangers' complex designs. They can account for up to 70% of CSP power cycle specific cost [8], which makes them a critical piece of equipment for sCO_2 and CO_2 mixture cycles. For recuperative heat exchangers of sCO_2 cycles printed circuit heat exchangers (PCHE) are usually considered in the literature. However, the cost difference between PCHE and non-PCHE is little [9] and the maximum thermal power of existing PCHE does not exceed 50 MWth with significant challenges in scale-up [10]. Therefore, shell and tube heat exchangers were considered for current high-power application (multiple hundred MWth range). This paper aims to identify a robust technological solution for the implementation of the above cycles in an industrial setup. This work is part of the EU-funded TOPCSP project, which aims to improve the design of the different systems of a CSP plant [11]. Estimation of performance of alternative equipment technologies upon heat transfer surface and material mass basis may provide additional insight to users and plant designers aimed at maximizing exchangers' cost reduction.

2. Methodology

The duty of heat exchangers was calculated to achieve the power cycle electric output of around 100 MWe based on a CSP with solar multiple of 2.4 and design power to the receiver of 670 MWth similar to Crescent Dunes plant according to SAM default solar tower CSP plant [12]. Both sCO_2 and CO_2+$SiCl_4$ mixture cycles were considered in recompression layout (RC) with the CO_2+$SiCl_4$ mixture also considered in the simple recuperated cycle (SC) at 550°C TIT and 250 bar maximum pressure. The mixture cycles parameters were optimized based on electrical efficiency with a minimum cycle temperature equal to 50°C [3]. For recompression and simple mixture cycles the working fluid molar composition (CO_2/$SiCl_4$) was chosen to be 91/9 and 80/20 respectively based on electrical efficiency optimization as can be seen in **Figure 1**. For the sCO_2 recompression cycle, the optimized minimum pressure was 110 bar with the recompression fraction equal to 0.286.

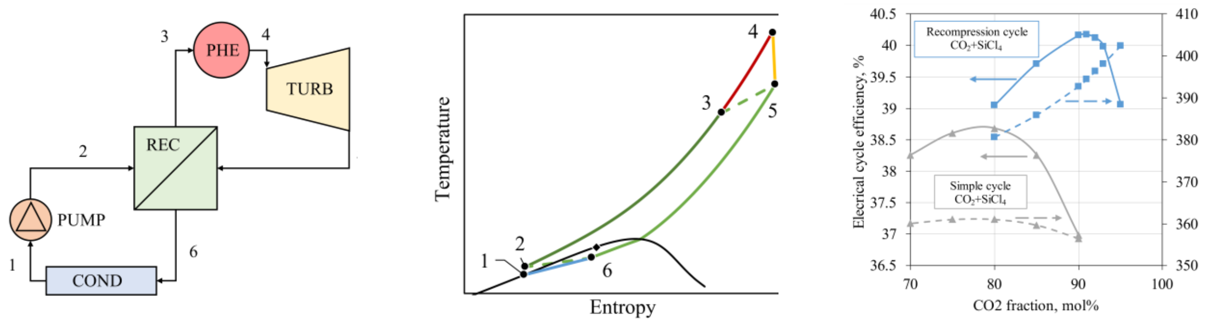

(a) **(b)** **(c)**

Figure 1. *Layout **(a)** and T-s diagram **(b)** of recuperated CO_2+$SiCl_4$ mixture simple cycle, **(c)** cycles electrical efficiency and PHE inlet temperature vs CO_2 molar fraction at 550°C TIT*

The properties of solar salt were calculated according to [13], while for calculating sCO_2 properties Span-Wagner EoS was used [14]. The CO_2+$SiCl_4$ mixture properties were calculated using Peng-Robinson EoS [15] and friction theory models [6], [7] with binary interaction parameter equal to 0.06098 [5]. The resulting properties tables were transferred to HTRI with 30 maximum allowable temperature steps and 5 bar pressure steps.

The primary heat exchanger (PHE) and recuperators, including high and low-temperature recuperators (HTR and LTR), have been designed in detail using the shell-and-tube heat exchanger (STHE) in conventional configuration and using the EMbaffle® technology [16]. The main advantages of EMbaffle® technology are due to the pure countercurrent flow, low shellside pressure drops, and no flow-induced vibrations. This leads to a more compact size of EMbaffle® technology under a wide range of process design conditions. The input parameters for heat exchanger designs are shown in **Table 1**. Pressure drops were assumed according to literature [5].

Table 1. *Heat exchangers design parameters*

Power cycle		sCO_2 RC			CO_2+SiCl_4 SC		CO_2+SiCl_4 RC		
Heat exchanger		PHE	HTR	LTR	PHE	Rec.	PHE	HTR	LTR
Duty, MWth		283	582	194	285	533	284	411	195
Hot side	Fluid	Salt	sCO_2		Salt	CO_2+SiCl_4	Salt	CO_2+SiCl_4	
	Flow, kg/s	1429	1748		989	1485	1197	1636	
	T_{in}/T_{out}, °C	570/441	457/175	175/112	570/381	426/93	570/414	435/193	193/94
	$P_{in}/\Delta P$, bar/%	5/10	116/1.5	114/1.5	5/10	75/1.5	5/10	88/1.5	87/1.5
Cold side	Fluid	sCO_2			CO_2+SiCl_4				
	Flow, kg/s	1748		1249	1485		1636		1187
	T_{in}/T_{out}, °C	421/550	170/421	90/170	361/550	74/361	394/550	188/394	87/188
	$P_{in}/\Delta P$, bar/%	249/2	249/0.3	250/0.3	249/2	250/0.3	249/2	249/0.3	250/0.3

All STHEs were designed according to TEMA standards [17] using HTRI v.9.1 [18]. The maximum weight of the bundle was assumed to be within 160 tons with a shell outer maximum diameter of 4 m due to transport limitations. The flow with the highest pressure was located on the tube side. The fouling resistance was assumed to be $1.76x10^{-4}$ m^2K/W on the solar salt side and $8.81x10^{-5}$ m^2K/W for the sCO_2 and CO_2 mixture side [19]. The tubes outside diameters were assumed to be equal to 15.875 mm or 5/8" for all cases. The mechanical design was performed according to Section VIII ASME Div.1 with PV Elite [20]. Adequate materials have been identified for the considered fluids. For PHE Alloy 625 was chosen for channels and tubesheets, SS347H for tubes and shell, while for HTR and LTR 9Cr and carbon steel (CS) were used respectively [21], [22], [23].

3. Results

The main criteria for heat exchanger comparison is usually heat transfer surface, which for many applications allows for accurate cost prediction [24]. However, in the case of CO_2 cycles high pressures and temperatures are present, which makes weight a better indicator of the final cost. Due to high pressures throughout the cycle heat exchanger parts, like channels, covers, and tubesheets, make a significant portion of the final heat exchanger weight. The weight of these elements depends among other parameters on the diameter of shells, which is determined by throughput area and therefore by the maximum accommodating volume flow, governed by the allowable pressure drop, the material availability and the fabrication technology constraints. The solar salt volume flow is below 1 m^3/s and is much smaller compared to the sCO_2 and CO_2+SiCl_4 mixture flows as can be seen in **Figure 2**. This is due to the similar heat capacity and the tenfold difference in density of cold and hot fluids which leads to the small pressure drop in the salt side.

The cold fluid mass flow in PHE is smaller in the case of mixture power cycles due to the lower temperature of the cold fluid at the PHE inlet (**Table 1**). The mixture of CO_2+$SiCl_4$ also has a higher density than sCO_2 in PHE conditions. These two effects lead to around 50 and 25% smaller volume flow in the case of mixture simple and recompression power cycles PHE and to smaller shell and channel diameters. The HTR and LTR heat exchangers hot side volume flows are not so sensitive to the fluid chemical composition because of the mixture lower pressure. However, HTR and LTR cold side volume flows are around 20-25% smaller for the CO_2+$SiCl_4$ recompression cycle compared to the sCO_2 one.

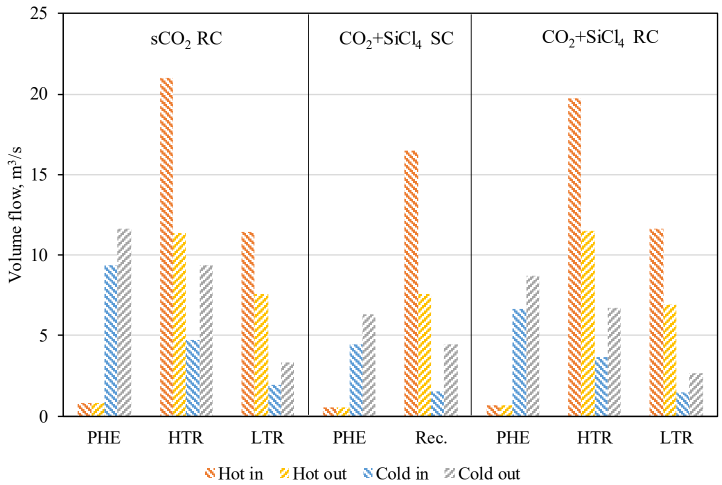

Figure 2. *Volume flows in heat exchangers*

The heat exchangers duty was calculated within 0.4% of the design value, while all pressure drops were within the allowed limits. In the case of conventional STHE, a No Tubes In Window (NTIW) baffle design with supports was adopted to prevent vibrations and reduce shell side pressure drop. The results of the STHE design are shown in **Table 2**.

Table 2. *Heat exchangers design results*

Power cycle			**sCO_2 RC**			**CO_2+$SiCl_4$ SC**		**CO_2+$SiCl_4$ RC**		
Heat exchanger			**PHE**	**HTR**	**LTR**	**PHE**	**Rec.**	**PHE**	**HTR**	**LTR**
Conventional	ΔP calc./ allow., bar	Hot	0.48/0.5	1.44/1.74	1.56/1.71	0.44/0.5	0.78/1.12	0.44/0.5	0.78/1.32	0.93/1.3
		Cold	4.17/4.97	0.55/0.75	0.46/0.75	4.28/4.97	0.53/0.75	4.87/4.97	0.64/0.75	0.67/0.75
	Parallel/series/(total)		2/2 (4)	5/3 (15)	4/3 (12)	2/3 (6)	5/4 (20)	2/3 (6)	6/3 (18)	5/4 (20)
	Shell ID, mm		2400	2550	2600	1900	2200	2150	2200	2550
	Eff. length, mm		14292	13950	14950	14049	15450	11532	12950	15800
	Total area, 10^3 m^2		18.07	75.20	97.70	16.97	82.68	17.57	53.78	113.88
Embaffle®	ΔP calc./ allow., bar	Hot	0.44/0.5	1.7/1.74	1.62/1.71	0.44/0.5	1.11/1.12	0.47/0.5	1.24/1.32	1.27/1.3
		Cold	4.75/4.97	0.55/0.75	0.57/0.75	4.87/4.97	0.73/0.75	4.67/4.97	0.7/0.75	0.73/0.75
	Parallel/series/(total)		2/2 (4)	4/3 (12)	3/4 (12)	1/3 (3)	2/4 (8)	1/2 (2)	2/3 (6)	3/4 (12)
	Shell ID, mm		1730	2100	2100	2150	2600	2200	2500	2200
	Eff. length, mm		14409	11250	12142	12674	11268	17542	9950	14580
	Total area, 10^3 m^2		16.64	58.16	62.77	17.18	60.33	16.63	36.86	82.91

As can be seen from **Figure 3** in the case of PHE due to the use of solar salt on the shell side relatively high heat transfer coefficients are seen in all cases which leads to similar heat exchange areas. In the case of recuperators, there is a significant increase in the shell side heat transfer coefficient due to the use of EMbaffle® technology.

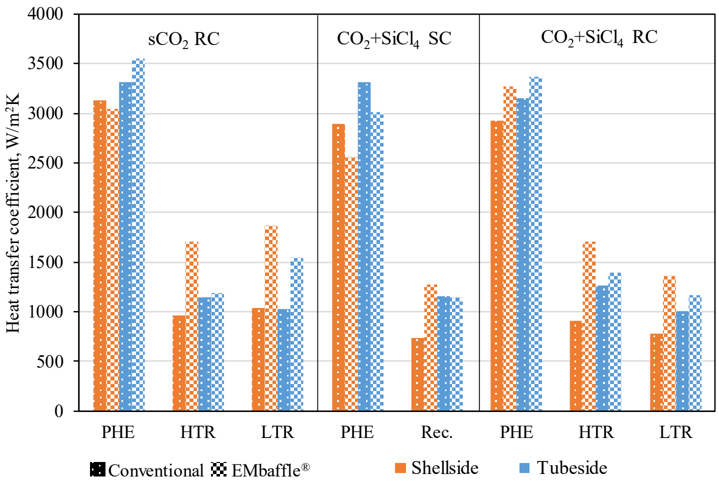

Figure 3. *The heat transfer coefficient of heat exchangers*

The product of effective area and heat transfer coefficient (UA) is used for cost estimation in multiple models for sCO_2 heat exchangers [9], therefore it was used in this study too. Notably, the dependence between the area and UA for EMbaffle® technology has a much lower slope compared to the conventional design as seen in **Figure 4**. In the case of recuperators, EMbaffle® technology has a clear advantage and consistently lower heat exchange area for the same UA. For PHE the area is very similar in all considered cases due to similar heat transfer coefficients. However, adopting the same number of shells in PHE, the EMbaffle® solution would allow for the reduction of the shell's internal diameter, which is important for the selected material use and transportation costs. Moreover, EMbaffle® versus NTIW optimized designs require fewer shells in most cases (**Figure 5**).

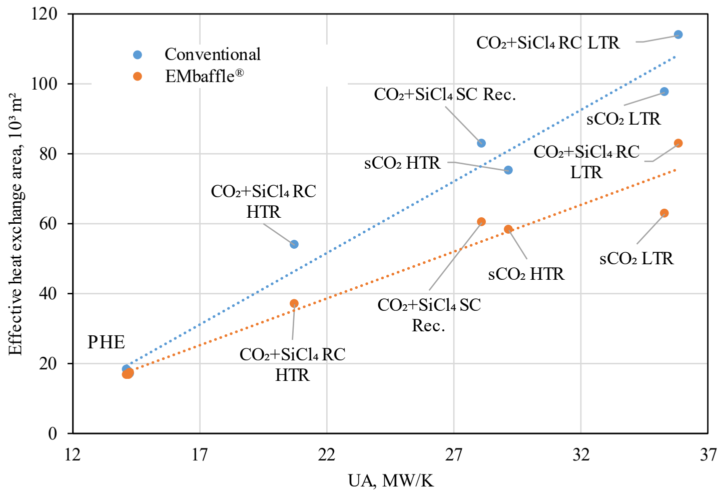

Figure 4. *The heat exchangers area vs UA*

The transition from sCO_2 to CO_2+$SiCl_4$ mixture cycles does not significantly change the PHE and recuperative system area. As can be seen from **Figure 5** in the case of a mixture recompression cycle the bigger part of the recuperative STHE area is represented by LTR, which is made from cheaper material. It is also important to mention the big deviation in the number of shells between conventional and EMbaffle® designs in the case of the recuperator and HTR for CO_2+$SiCl_4$ mixture cycles. Due to the vibrations occurring in the shell side, the flow speed is limited, which leads to underutilization of hot stream pressure drop and higher than expected heat exchange area.

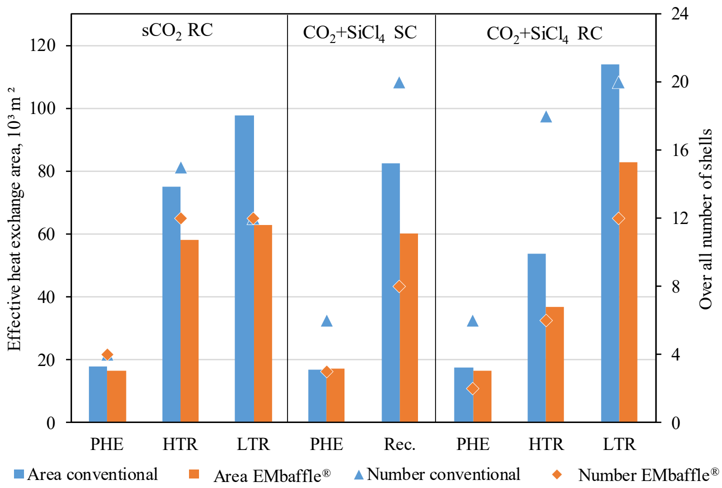

Figure 5. *The area and number of shells of heat exchangers*

The results of the mechanical design for a single shell are shown in **Figure 6**. In the case of sCO_2, as the number of shells is similar in both designs, the weight of the EMbaffle® single shell is lower. Moving to mixtures, although the single shell with conventional design becomes lighter, the total number of shells significantly increases compared to EMbaffle. The higher heat transfer rate and the larger accommodated surface per shell diameter of the EMbaffle technology lead to the higher contribution of tubes in the single shell weight in all considered cases. This means that a bigger percentage of materials is spent on heat exchange surfaces, which leads to significant savings in high-temperature applications such as PHE.

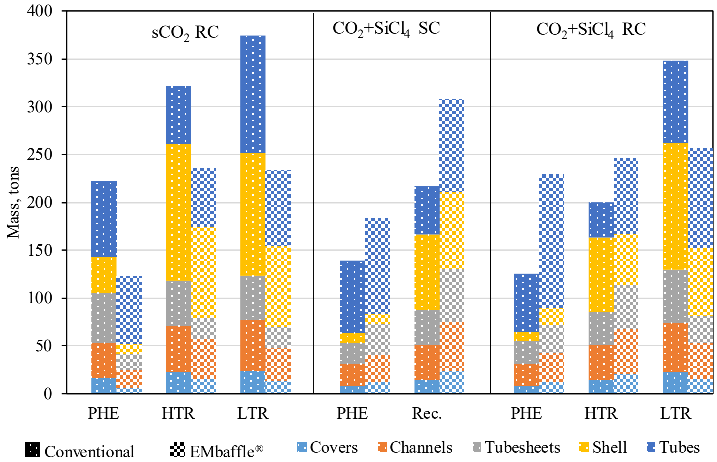

***Figure 6.** The weight distribution of one shell components*

The total weights of the heat exchangers considered are shown in **Figure 7**. One can see a significant weight reduction using EMbaffle® technology, especially for recuperative systems. The difference between the technologies increases with the UA as it was in the case of the area dependence on the UA shown in **Figure 4**. This will lead to the overestimation of cost correlations based on conventional STHE UA. However, the weight savings moving to EMbaffle® grow faster than area savings, which is determined by the higher material percentage being spent on tubes, meaning heat exchange surface (as shown in **Figure 6**).

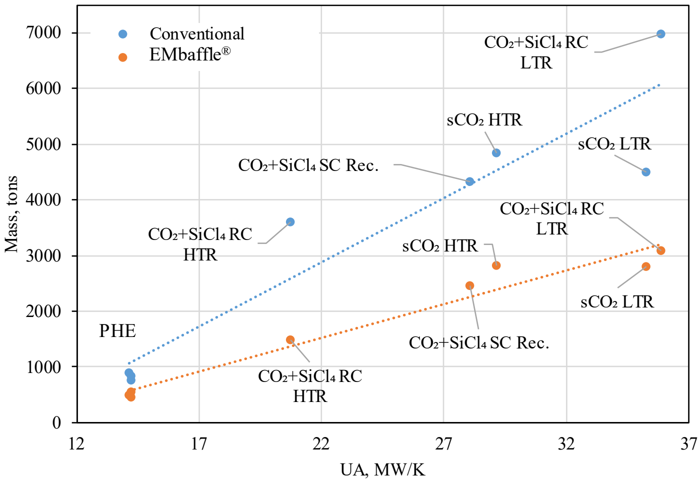

***Figure 7.** Heat exchangers mass against the UA*

The material saving is especially important in the case of PHE since it uses an expensive nickel-based alloy 625. Using the EMbaffle® leads to the reduction of Alloy 625 and 347H use by 61 and 28% in the case of sCO_2 PHE, 31 and 36% for CO_2+$SiCl_4$ simple cycle PHE, 56 and 27% for CO_2+$SiCl_4$ recompression cycle PHE (Figure 7). For the recuperative system, the weight reduction is 37 and 41% for sCO_2 low and high temperature parts respectively, 44% for the recuperator, 56 and 59% for CO_2+$SiCl_4$ LTR and HTR.

There is a 15% and 6% reduction in PHE weight mass using conventional and EMbaffle® design, with 24 and 14% reduction in Alloy 625 weight moving from sCO_2 to CO_2+$SiCl_4$ mixture in the recompression cycle. This is due to the mixture's lower volume flow as shown in **Figure 2**, which leads to a lower throughput area, meaning fewer shells in parallel or smaller shell diameters. For HTR the mass reduction is 24 and 47% for conventional and EMbaffle® designs and is due to the heat exchange area reduction of 28 and 36% respectively. In the case of

LTR, the use of a mixture leads to the increase of weight by 56 and 10% for conventional and EMbaffle® designs, while the area increases by 16 and 32% respectively. Since 9Cr-1Mo steel used in HTR is more expensive than carbon steel in LTR, the final cost of the recuperative system could be similar or lower in the case of the CO_2+$SiCl_4$ mixture recompression cycle.

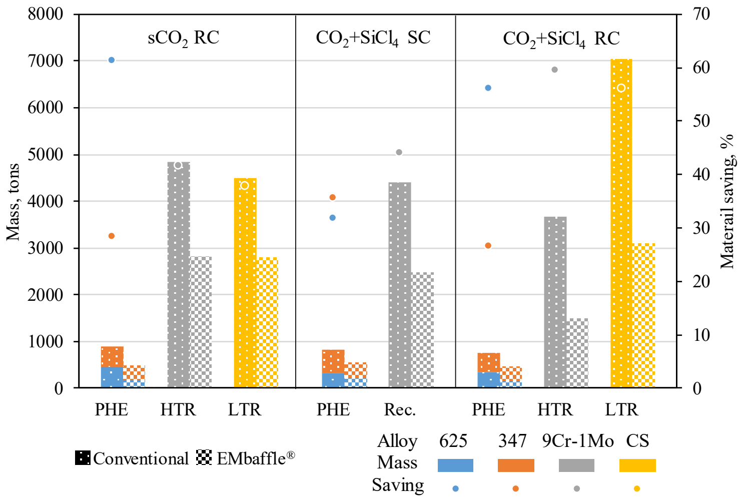

Figure 8. *The material mass distribution of heat exchangers*

4. Conclusions

In this paper shell and tube heat exchanger implementation for sCO_2 and CO_2+$SiCl_4$ cycles was investigated. Materials were chosen and thermal design followed by mechanical design was carried out to determine the heat exchange area, number of shells, weight of components, and materials used.

In the case of primary heat exchangers, the effective heat exchange area is almost the same for all considered technologies and cycles; however, by using EMbaffle® one can get smaller diameter shells maintaining the same pressure drop and lack of vibrations. For recuperators, the use of EMbaffle® allows for a smaller effective heat exchange area and smaller throughput area which translates to smaller shell diameters or fewer shells used. Therefore, in all cases, the use of EMbaffle® technology leads to lower weight in expensive alloys.

All considered primary heat exchangers have a similar UA and area. However, due to the lower mass flow and higher density of the CO_2+$SiCl_4$ mixture compared to sCO_2 the throughput area and therefore number of shells in parallel or shell diameter are smaller in mixture cycles. This leads to the reduction of recompression cycle primary heat exchanger weight by 15 and 6% using conventional and EMbaffle® technology, with 24 and 14% reduction in Alloy 625. The transition from sCO_2 to CO_2+$SiCl_4$ in the recompression cycle leads to the redistribution of UA, area, and weight from the high-temperature recuperator to the low-temperature recuperator, which will lead to a similar or smaller overall cost or recuperative system.

Additional experimental investigation of enhanced-tubes geometries in EMbaffle® heat exchangers is ongoing at the B&R industrial site to validate performance over pressure drops improvement for next deployments.

Data availability statement

Data is not presented in this article. Further information about the heat exchangers designs is available upon request.

Author contributions

Vladimir Naumov: Investigation, Visualization, Writing – original draft. Marta Mantegazza: Investigation, Software, Methodology. Michele Doninelli: Investigation. Gioele Di Marcoberardino: Supervision, Writing – review & editing. Paolo Iora: Project administration, Supervision, Conceptualization. Marco Rottoli: Methodology, Supervision, Writing – review & editing.

Competing interests

The authors declare that they have no competing interests.

Funding

This paper is part of the TOPCSP project that has received funding from the European Union's HORIZON MSCA Doctoral Network, Project number 101072537.

Acknowledgement

We would like to thank GianLuca Anfossi for the contribution to the mechanical design of the heat exchangers and Marcello Garavaglia for the contribution to results analysis and editing.

References

[1] "Renewable power generation costs in 2021," IRENA, Abu Dhabi, 2022.
[2] V. Dostal, M. J. Driscoll, P. Hejzlar, and Y. Wang, "Supercritical CO2 Cycle for Fast Gas-Cooled Reactors," in *Volume 7: Turbo Expo 2004*, Vienna, Austria: ASMEDC, Jan. 2004, pp. 683–692. doi: 10.1115/GT2004-54242.
[3] F. Crespi *et al.*, "Thermal efficiency gains enabled by using CO2 mixtures in supercritical power cycles," *Energy*, vol. 238, p. 121899, Jan. 2022, doi: 10.1016/j.energy.2021.121899.
[4] M. Nakayama *et al.*, "Thermal decomposition of tetrabromosilane and deposition of crystalline silicon," *Materials Science in Semiconductor Processing*, vol. 23, pp. 93–97, Jul. 2014, doi: 10.1016/j.mssp.2014.02.045.
[5] M. Doninelli *et al.*, "Experimental investigation of the CO2+SiCl4 mixture as innovative working fluid for power cycles: Bubble points and liquid density measurements," *Energy*, p. 131197, Apr. 2024, doi: 10.1016/j.energy.2024.131197.
[6] S. E. Quiñones-Cisneros, C. K. Zéberg-Mikkelsen, and E. H. Stenby, "One parameter friction theory models for viscosity," *Fluid Ph. Equilib.*, vol. 178, no. 1–2, pp. 1–16, Mar. 2001, doi: 10.1016/S0378-3812(00)00474-X.
[7] S. E. Quiñones-Cisneros, S. Pollak, and K. A. G. Schmidt, "Friction Theory Model for Thermal Conductivity," *J. Chem. Eng. Data*, vol. 66, no. 11, pp. 4215–4227, Nov. 2021, doi: 10.1021/acs.jced.1c00400.
[8] G. Manzolini *et al.*, "Adoption of CO2 blended with C6F6 as working fluid in CSP plants," presented at the SOLARPACES 2020: 26th International Conference on Concentrating Solar Power and Chemical Energy Systems, Freiburg, Germany, 2022, p. 090005. doi: 10.1063/5.0086520.
[9] N. T. Weiland, B. W. Lance, and S. R. Pidaparti, "sCO2 Power Cycle Component Cost Correlations From DOE Data Spanning Multiple Scales and Applications," in *Volume 9: Oil and Gas Applications; Supercritical CO2 Power Cycles; Wind Energy*, Phoenix, Arizona, USA: American Society of Mechanical Engineers, Jun. 2019, p. V009T38A008. doi: 10.1115/GT2019-90493.
[10] B. Lariviere *et al.*, "sCO2 power cycle development and STEP Demo pilot project," *Conference Proceedings of the European sCO2 Conference4th European sCO2 Conference*

for Energy Systems: March 23-24, vol. 2021, p. 352, Mar. 2021, doi: 10.17185/DUEPUB-LICO/73979.

[11] "Doctoral Network | TOPCSP." Accessed: Apr. 24, 2024. [Online]. Available: https://topcsp.eu/

[12] F. D. Andalucia, "System advisor model (SAM) case study: Gemasolar," *Nrel, Case Report*, pp. 1–10, 2013.

[13] H. Benoit, L. Spreafico, D. Gauthier, and G. Flamant, "Review of heat transfer fluids in tube-receivers used in concentrating solar thermal systems: Properties and heat transfer coefficients," *Renewable and Sustainable Energy Reviews*, vol. 55, pp. 298–315, Mar. 2016, doi: 10.1016/j.rser.2015.10.059.

[14] R. Span and W. Wagner, "A New Equation of State for Carbon Dioxide Covering the Fluid Region from the Triple‐Point Temperature to 1100 K at Pressures up to 800 MPa," *J. Phys. Chem. Ref. Data*, vol. 25, no. 6, pp. 1509–1596, Nov. 1996, doi: 10.1063/1.555991.

[15] D.-Y. Peng and D. B. Robinson, "A New Two-Constant Equation of State," *Ind. Eng. Chem. Fund.*, vol. 15, no. 1, pp. 59–64, Feb. 1976, doi: 10.1021/i160057a011.

[16] M. Rottoli, T. Odry, D. Agazzi, and E. Notarbartolo, "EMbaffle® Heat Exchange Technology," *Innovative Heat Exchangers*, pp. 341–361, 2018.

[17] R. C. Byrne, "Standards of the Tubular Exchanger Manufacturers Association, Tenth Edition," TEMA.

[18] "Xist." Accessed: Mar. 21, 2024. [Online]. Available: https://www.htri.net/xist

[19] "Investigation of thermal storage and steam generator issues," SAND--93-7084, 10189397, ON: DE94001558, Aug. 1993. doi: 10.2172/10189397.

[20] "PV Elite®," Hexagon. Accessed: Apr. 05, 2024. [Online]. Available: https://hexagon.com/it/products/pv-elite

[21] B. A. Pint, R. Pillai, and J. R. Keiser, "Defining Temperature Limitations for Steels in sCO2 Applications".

[22] K. Li, Z. Zhu, B. Xiao, J.-L. Luo, and N. Zhang, "State of the art overview material degradation in high-temperature supercritical CO2 environments," *Progress in Materials Science*, vol. 136, p. 101107, Jul. 2023, doi: 10.1016/j.pmatsci.2023.101107.

[23] R. Moore, N. Siegel, G. Kolb, M. Vernon, and C. Ho, "Design considerations for concentrating solar power tower systems employing molten salt.," SAND2010-6978, 1008140, Sep. 2010. doi: 10.2172/1008140.

[24] M. Taal, "Cost estimation and energy price forecasts for economic evaluation of retrofit projects," *Applied Thermal Engineering*, vol. 23, no. 14, pp. 1819–1835, Oct. 2003, doi: 10.1016/S1359-4311(03)00136-4.